J. Earth Planet. Sci. Nagoya Univ., Vol. 59, 1 to 15, 2012

# Enhanced dissolution of soda-lime glass under stressed conditions with small effective stress (0.05 MPa) at 35°C to 55°C: Implication for seismogeochemical monitoring

**Kazuya MIYAKAWA[1*], Tianshi YANG and Iwao KAWABE**

[1]*Department of Earth and Planetary Sciences, Graduate School of Environmental Studies, Nagoya University, Furo-cho, Chikusa, Nagoya 464-8601, Japan*
(Received October 15, 2012 / Accepted December 7, 2012)

## ABSTRACT

Dissolution rates of pressure solution (PS) of $SiO_2$ of soda-lime glass in 0.002 M $NaHCO_3$ solution were experimentally determined at low temperatures (35°C to 55°C) and low effective stresses (0.05 MPa). They were $18 \pm 2 \times 10^{-15}$ (35°C), $49 \pm 4 \times 10^{-15}$ (45°C) and $133 \pm 17 \times 10^{-15}$ (55°C) (Si mol/cm$^2$/sec), respectively. The ratios of the dissolution rates of stressed glasses to those of glass beads at zero effective stress were 1.5 ± 0.5 (35°C), 1.5 ± 0.4 (45°C) and 1.4 ± 0.6 (55°C), respectively, which means that the stressed glasses dissolve about 1.5 times as fast as glasses at zero effective stress. In response to a step-like increase of applied uniaxial loads, the dissolution rates of PS increased immediately, but the dissolution rate decreased gradually in the course of keeping the effective stress constant. The apparent activation energy of our PS experiments was calculated to be approximately (78 ± 12) kJ/mol, and this value is slightly smaller than (89 ± 1) kJ/mol of dissolution reaction of soda-lime glass at effective stress = 0. Our results clearly show that even at such low temperatures and low effective stresses, Si release into solution as a result of PS can be detected.
**Keywords.** pressure solution, silica dissolution, earthquake prediction

## 1. INTRODUCTION

Pressure solution (PS) is a process by which materials can be dissolved at intergranular or intercrystalline contacts under high stress and precipitated at interfaces under low stress. In geological disposal systems for nuclear wastes, PS has been considered as an important process of material release of radioactive waste into geological environment (Ichikawa *et al.*, 2011). However, to date, the understanding of the PS reaction of glass has been limited.

The parameters controlling PS reaction have been studied by many researchers as regard to crystalline silica dissolution (de Boer, 1977a, 1977b; Schutjens, 1991; Shimizu, 1995; Dewers and Hajash, 1995; Renard *et al.*, 1999; He *et al.*, 2003, 2007; Bernabé *et al.*, 2009). Since PS phenomena have been reported in low grade metamorphic rocks with temperature ranging from 150°C to 350°C such as greenschist facies (McClay, 1977), intensive studies on the behavior of PS of quartz at relatively high temperature and high differential stress have been carried out. However, there is no experimental study

*Corresponding author, e-mail: kazuya_miyakawa@nagoya-u.jp (K. Miyakawa)
Tel: +81 1632-5-2022, Fax: +81 1632-5-2344

on PS at low temperature and low effective stress conditions, possibly because the PS process has been thought to have little influence on the deformation of sedimentary rocks at low temperature and low effective stress.

The purpose of this study is to make it clear whether PS phenomenon could significantly enhance the dissolution rate of glass or quartz even at low temperature and low differential stress, or not. In an open natural system, the dissolved silica due to PS is expected to be transferred into groundwater-flow by pore-fluid flow without immediate re-precipitation. The deformation or movement of crustal rocks, which is closely related to the earthquake, can change the stress condition of the shallow crustal rocks. In such a case, an increase in differential stress will highly promote the PS reaction at grain contacts. As a result, Si concentration in groundwater is to be changed due to PS reaction. Therefore, there is a possibility that the accumulation of the differential stress in the shallow crust may be detected by means of monitoring the Si concentration in the groundwater in cracked media of crystalline rocks. Our goal of this study is to formulate a new geochemical method for earthquake prediction based on the PS phenomenon of granitic rock.

In order to evaluate this possibility, it is necessary to investigate the effects of PS on Si release at low temperature and low effective stress. Stress drops in crustal earthquakes are in the range of 1 – 10 MPa (Scholz, 2002), although the transient crustal stress resulting from solid earth tides is in an order of magnitude of hPa. If the crustal stress condition changes prior to a large earthquake, the magnitude of stress changes will fall in between these two cases. Hence, we will examine the PS behavior in the range of 0.1 – 1 MPa.

Amorphous silica has larger solubility in water compared to crystalline silica. Accordingly, glass is expected to dissolve faster than quartz even when subjected to the small stress. In the present work, we will report the rates of dissolution and PS reaction of soda-lime glass as a function of temperature at pH 8 to 9.

## 2. EXPERIMENTAL METHOD

Schematic illustration of experimental apparatus is shown in Fig. 1(a). Teflon beakers were put into a temperature-controlled water bath with a thermostat (SJ-10R, TAITEC Co.). Reactors made of rigid polyvinyl chloride (PVC) pipe, in which soda-lime-glass beads were put, were placed in the Teflon beakers. There are small holes in sidewalls of each reactor in order to circulate a pore solution. The $NaHCO_3$ solution ($2 \times 10^{-3}$ M) of 450 ml was put into the each Teflon beaker. The solution was circulated by a peristaltic pump (MP-1000, Tokyo Rikakikai Co. Ltd.) with a plastic tube one end of which is inserted into glass beads of the reactor. The solution steadily flows through the pore space of sample grains by a low circulating rate of 0.5 – 1 ml/min (Fig. 1(b)). Because of the circulation of the pore solution, the dissolution reaction was not the diffusion-controlled reaction but reaction-controlled one. The circulation of pore solution enables us to detect an influence of PS reaction in a short experimental period.

Two types of dissolution runs were conducted in parallel. First one is a PS experiment where an effective stress is applied to the quartz grains, and the other

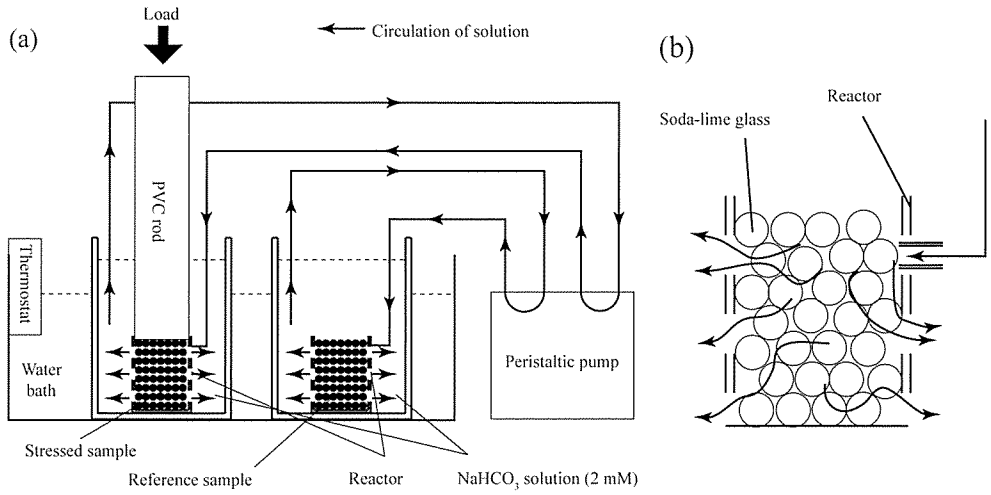


**Fig. 1:** (a) Schematic illustration of experimental apparatus. (b) Enlarged illustration of the reactor. Curves with arrows indicate the circulation of solution.

is a dissolution experiment where the glass beads dissolve at zero effective stress. The procedure of the PS experiment was as follows. After dissolution experiments in unstressed conditions, which lasted for 170 – 290 hrs, stresses were applied to the glass beads by putting a weight on the PVC rod. The applied stresses were kept constant for 190 – 240 hrs, and then the applied stresses were removed. These increases and decreases of applied stresses were a step-like function of time. At the last stress-free conditions, the dissolution experiments continued. Hereafter, these soda-lime-glass grains used in the PS experiments are referred to as "stressed sample".

The dissolution experiments of the glass beads at zero effective stress were conducted concurrently with the PS experiments described above. In this experiment, glass beads were dissolved only with circulation of pore solution. Hereafter, these glass beads used in this dissolution experiments are referred to as "reference sample", dissolution behaviors of which are compared with those of the stressed samples.

### 2.1. Sample preparation

The grain size of soda-lime glass used in our experiments ranged from 1.5 – 2.0 mm. The chemical composition of this soda-lime glass was determined as follows (Yang, 2011): the glass beads were pulverized and dissolved by HF-HCl-$HClO_4$ mixtures, and then, the solutions were analyzed for Na, Ca, Mg, and Al by inductively coupled plasma atomic emission spectroscopy (ICP-AES). $SiO_2$ concentration was obtained by subtracting the sum of the concentrations of every oxide ($Na_2O$, CaO, MgO, and $Al_2O_3$) from 100%. The result was as follows (wt %): $SiO_2$ = 73.84 ± 0.21 %, $Na_2O$ = 12.73 ± 0.20 %, CaO = 9.04 ± 0.05 %, MgO = 3.57 ± 0.04 %, and $Al_2O_3$ = 0.82 ± 0.02 %, where the errors are 1 sigma (n = 3). Starting materials were washed ultrasonically with distilled water for 2 – 3 hrs, then, dried at 40°C for 1 – 2 days in order to remove disturbed surface layers and ultrafine particles.

**Table 1** Experimental conditions for soda-lime glass.

| Temperature (°C) | Stressed or reference #1 | Amount of soda-lime glass (g) | Confined pressure (MPa) | Effective stress (MPa) | Initial pH | Final pH | Calculated surface area ($m^2$) #2 |
|---|---|---|---|---|---|---|---|
| 35 | St. | 18.3 | 0.1 | 0.05 | 8.47 | 8.75 | $2.6 \times 10^{-2}$ |
| 35 | Ref. | 18.0 | 0.1 | 0 | 8.37 | 8.76 | $2.6 \times 10^{-2}$ |
| 45 | St. | 19.1 | 0.1 | 0.05 | 8.32 | 8.91 | $2.7 \times 10^{-2}$ |
| 45 | Ref. | 19.0 | 0.1 | 0 | 8.26 | 8.84 | $2.7 \times 10^{-2}$ |
| 55 | St. | 19.5 | 0.1 | 0.05 | 8.75 | 9.34 | $2.8 \times 10^{-2}$ |
| 55 | Ref. | 19.5 | 0.1 | 0 | 8.75 | 9.28 | $2.8 \times 10^{-2}$ |

#1 "Stressed sample system" and "reference sample system" are denoted as "St." and "Ref.", respectively.

#2 The suraface area ($A$) of soda-lime-glass grains is geometrically calculated on the assumption that $A = 3Wr^{-1}\rho^{-1}$ as in section 2.1, where W denotes the amount of soda-lime glass, r is radius of grain, and ρ represents the density of glass.

The surface area of glass sample was geometrically calculated on the assumption that sample grain is a sphere with a radius of r. The surface area ($A$) to volume ($V$) ratio of those close-packed spheres can be expressed as $A/V = 3/r$. Therefore, the surface area can be estimated as $A = 3Wr^{-1}\rho^{-1}$ in which $W$ denotes the mass of glass beads, and ρ represents the density of glass. The surface areas ($cm^2$) of glass samples are summarized in Table 1.

### 2.2. Experimental conditions

The experiments were carried out for three times with different temperatures. All the experiments were conducted at 1 atm. The value of the applied stress was calculated from an applied load divided by the cross-sectional area of the reactor. The effective stress ($\sigma_e$) was calculated as follows: $\sigma_e = \sigma - P$ ($\sigma$: applied stress, $P$: the ambient atmospheric pressure). The dilute $NaHCO_3$ solution (0.002 M) was used in all the experiments because of its pH value and buffering action. An initial pH and a final pH of the solution were determined before and after each experiment with a pH meter equipped with a glass electrode (D-13, HORIBA Ltd.). The accuracy of the pH meter is 0.02 pH unit. The experimental conditions of soda-lime glass dissolutions are summarized in Table 1.

### 2.3. Sampling and Analytical method

A small aliquot (approximately 1 ml) of the solution was collected for analysis once a day using a plastic syringe. The collected sample was filtered through a 0.20 μm Teflon filter (DISMIC-13HP, Toyo Roshi Kaisha Ltd.), and diluted with distilled water, finally placed into a Teflon bottle maintained at the same temperature of each experiment. The samplings of the solutions from stressed sample system and reference sample system were carried out at the same time.

Dissolved total Si concentration in each sampled solution was determined using Seiko SPS-1500R ICP-AES spectrometer. The limit of ICP-AES determination with

respect to Si is approximately 5 ppb.

## 3. RESULTS

The total Si concentration curves (mol/kg) in the both experiments of the stressed samples and the reference samples of soda-lime glass at 35°C, 45°C and 55°C are shown as a function of elapsed time in Fig. 2(a), (b) and (c), respectively. Similar dissolution experiments without and with stress were also made at 25°C (Yang, 2011), but the time-series data of dissolved Si concentrations show somewhat greater fluctuations than those in the other runs at 35°C, 45°C and 55°C. The runs at 25°C were preliminarily made in the initial stage of our study where we were not yet experienced. We omit results of the runs at 25°C.

The timings of applying loads and removal of loads are indicated with vertical broken lines in Fig. 2. The elapsed time of 0 represents the start of each experiment. Before applying the loads, the Si concentrations of the stressed sample system showed good agreement with those of the reference sample system at each temperature. After applying the loads, the Si concentration of the stressed sample system increased rapidly than the reference sample system. As regard to the results at 45°C and 55°C, even after removing the loads, the Si concentration of the stressed sample system appeared to increase faster than the reference sample system.

In order to eliminate the influences arising from the differences of total amounts of samples, the Si concentration differences between the stressed sample and the reference sample systems were divided by surface areas, and then plotted against the elapsed time for each temperature in Fig. 3(a), (b) and (c), respectively. During the period before the loading stress was applied, the Si concentration differences were nearly zero. This is indicative of the identical behavior of the each experimental system at zero effective stress. This result ensures that the increases of the Si concentration difference in Fig. 3 could be derived only from the effect of applied loads. However, the fluctuations of the results before applying loads were large especially in Fig. 3(a) although the analytical errors were small. These fluctuations may be due to a formation of a precipitate of a metal silicate because of impurities in the soda-lime glass. Figure 4 shows SEM photomicrographs of a stressed sample at 35°C, where some formations of precipitates are recognized around the grain contact. However, it is not always the case that precipitates are formed around every contact point in every experiment. After applying the stress, the Si dissolution was enhanced at each temperature. After the stress was removed, the graphs of Fig. 3 (b) and (c) showed positive slopes, but in Fig. 3(a), there was no obvious slope after the removal of the loading.

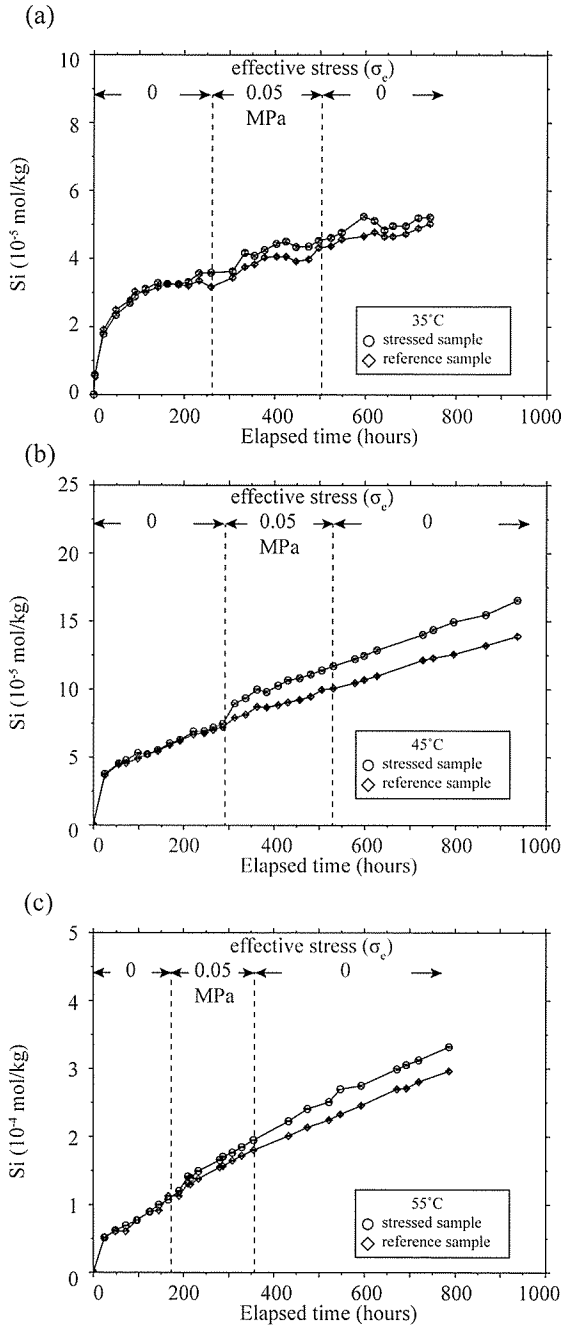


**Fig. 2:** Si concentration (mol/kg) as a function of elapsed time at 35°C (a), 45°C (b), and 55°C (c). *Circles* represent the stressed samples. *Diamonds* represent the reference samples. Two vertical broken lines indicate the timings of the application and the removal of the load in the stressed sample systems, respectively. Error bars represent 2 σ of standard error.

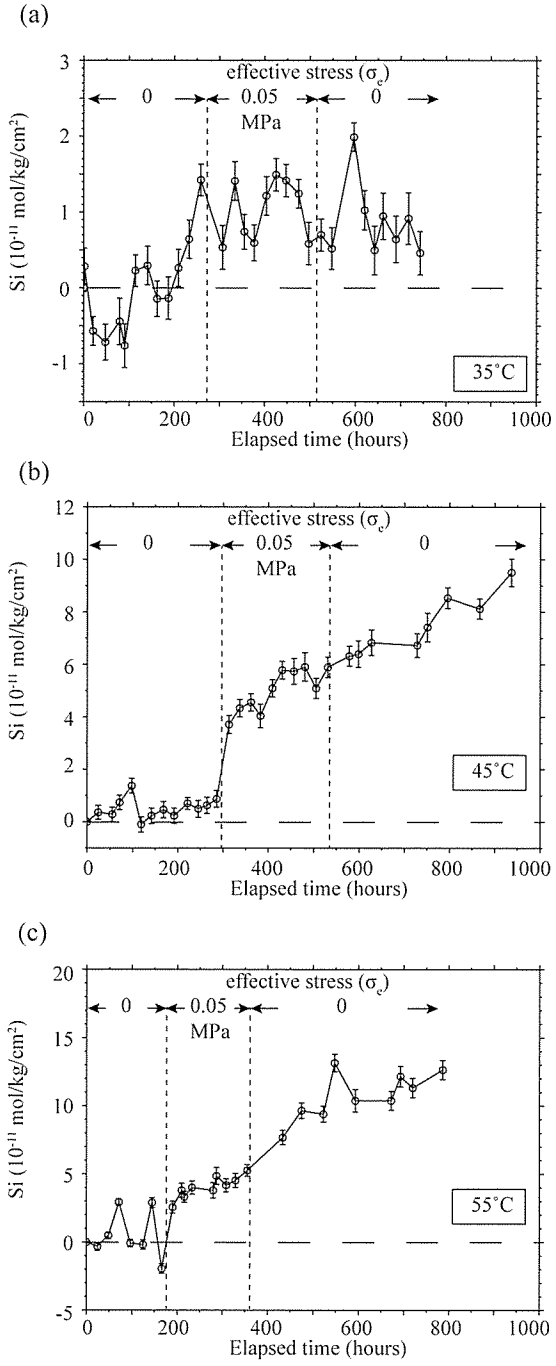


**Fig. 3:** Differences of the Si concentration per unit surface area (mol/kg/cm$^2$) between the stressed samples and the reference samples as a function of elapsed time. Two vertical broken lines indicate the timings of the application and the removal of the load in the stressed sample systems, respectively. Error bars represent 2 σ of standard error.

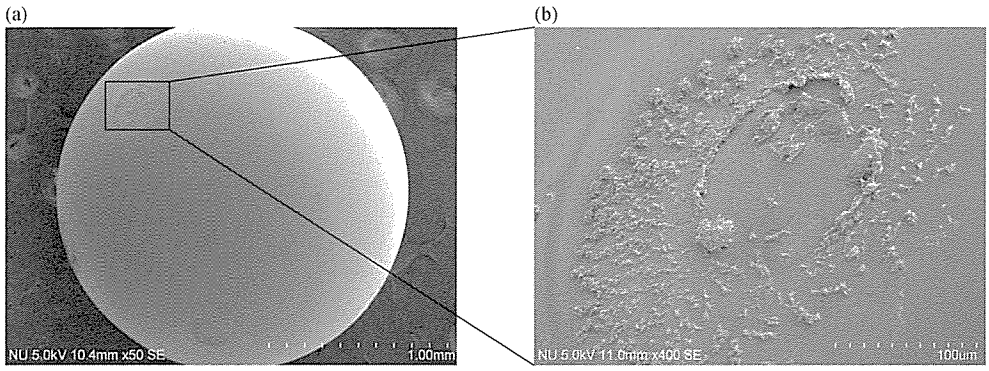


**Fig. 4:** SEM photomicrographs showing (a) grain surface of stressed sample at 35°C and (b) magnified area of the contact surface in (a) using Hitachi SU6600. Sample surfaces were coated with Au using Hitachi E-1045 ion spatter.

## 4. DISCUSSION

In this section, we will calculate the dissolution rate of soda-lime glass and the activation energy of PS reaction. The dissolution reaction of silica in alkaline solution can be represented by the equation:

$$SiO_2(s) + 2H_2O(l) = H_4SiO_4(aq)$$

In dissolution/precipitation reactions of silica under far from equilibrium condition, the precipitation rate is considered to be negligible when compared with the dissolution rate. In this case, the Si concentration as a function of time can be treated as the dissolution rate:

$$\text{Rate}_+ = \frac{dm_{H_4SiO_4}}{dt} \tag{1}$$

where the subscript + represents dissolution, $m$ is the silica concentration in solution, and $t$ denotes time. The dimension of the rate of Eq. (1) is mol/kg/sec. On the assumption that temperature, reactive surface area and the mass of solution are constant, the dissolution rate can be given in the form,

$$\frac{dm_{H_4SiO_4}}{dt} = \frac{A}{M} k_+$$

where $A$ and $M$ denote the interfacial area between sample grains and solution and the mass of solution, respectively. $k_+$ denotes the intrinsic rate constant of dissolution with the dimension of mol/cm$^2$/sec. As suggested by Rimstidt and Barnes (1980), $A/M$ represents the extent of the system which will be selected as the standard system with one square meter of interfacial area and 1 kg of water. They considered two basic requirements of kinetics: (1) The reaction rate between two phases is directly proportional to the interfacial area ($A$) between the phases, and (2) for a fixed volume of solute, the rate at which the concentration increases in a system is inversely proportional to the mass of water ($M$) in the system. However, in our experiment, we

cannot regard the mass of solution as constant because the mass of solution decreases with every sampling. In this paper, we calculated the dissolution rate by regarding the mass of water as variable, and the calculation procedure of the dissolution rate in the case of the decreasing mass of solution by sampling is described as follows.

### 4.1. Calculation with decreasing solution mass

A method for calculating dissolution rate in the case where the mass of water is decreased by the repetition of solution sampling is described here. Following Rimstidt and Barnes (1980), a rate equation based on transition state theory (Eyring, 1935) was derived to express the measured rates in terms of the activities of reacting substances for silica-water system (Eqns. 23 and 24 in Rimstidt and Barnes, 1980).

$$\left(\frac{\partial n_{H_4SiO_4}}{\partial t}\right)_{P,T} = M\left(\frac{\partial m_{H_4SiO_4}}{\partial t}\right)_{P,T,M} + m_{H_4SiO_4}\left(\frac{\partial M}{\partial t}\right)_{P,T,m}$$

$$= A\left(k_+ a_{SiO_2} a_{H_2O}^2 - k_- a_{H_4SiO_4}\right) \tag{2}$$

where $n$ is the mole number (mol) of silica in solution, $t$ is the reaction time (sec), $P$ is the pressure, $T$ is the temperature (K), $M$ is the mass of the solution (kg), $m$ is the silica concentration (mol/kg) in the solution, $A$ is the reactive surface area ($cm^2$), and $k$ is the rate constant ($mol/cm^2/sec$). The subscript + means the dissolution reaction, the subscript – denotes the precipitation reaction, and $a$ is the activity. In dilute aqueous solution,

$$a_{SiO_2} a_{H_2O}^2 \approx 1 \tag{3}$$

$$a_{H_4SiO_4} = m_{H_4SiO_4} \tag{4}$$

In dissolution/precipitation reactions of silica component far from equilibrium, the precipitation rate can be considered as negligibly small when compared with dissolution rate.

$$k_- a_{H_4SiO_4} = 0 \quad \left(k_+ >> k_- a_{H_4SiO_4}\right) \tag{5}$$

When the sampled volume of solution and the sampling frequency are constant, the mass of solution as a function of time can be approximated by

$$M = bt + M_0 \tag{6}$$

where $b$ is a negative coefficient and $M_0$ is the initial mass of solution. Substituting Eqs (3)–(6) into Eq. (2) gives

$$\frac{dm_{H_4SiO_4}}{dt} + \frac{b}{M} m_{H_4SiO_4} = \frac{Ak_+}{M} \tag{7}$$

Eq. (7) has the same form of an inhomogeneous ordinary differential equation as $y' + p(t)y = g(t)$. Using the method of variation of constants, the solution of Eq. (7) is given by

$$\frac{m_{H_4SiO_4}}{A} e^{\int \frac{b}{M} dt} = k_+ \int \frac{1}{M} e^{\int \frac{b}{M} dt} dt + \frac{m_0}{A} \tag{8}$$

where $m_0$ is the initial concentration of silica in solution. Plotting $\frac{m_{H_4SiO_4}}{A} e^{\int \frac{b}{M} dt}$ vs. $\int \frac{1}{M} e^{\int \frac{b}{M} dt} dt$ gives the intercept of $\frac{m_0}{A}$ (mol/kg/cm$^2$) and the slope of $k_+$ (mol/cm$^2$/sec). The dissolution rate constant can be obtained by fitting the experimental data to Eq. (8) using the method of weighted least squares. As an example, a conceptual fitting to Eq. (8) was illustrated in Fig. 5.

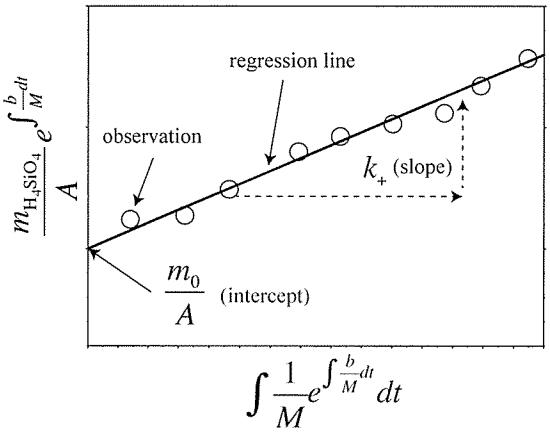


**Fig. 5:** Conceptual diagram for determination of the rate constant $k_+$ in Eq. (8). The rate constant can be obtained from observation plots using least-square fitting. $t$ is the reaction time (sec), $b$ is a negative coefficient, $M$ is the mass of the solution (kg), $m$ is the silica concentration (mol/kg) in the solution, $A$ is the reactive surface area (cm$^2$), and $k_+$ is the rate constant (mol/cm$^2$/sec).

Next, the calculation method for dissolution rate of PS from the difference in the Si concentration between the stressed sample and the reference sample is described. With Eq. (8), the difference in the silica concentration per unit surface area between the stressed sample and the reference sample systems can be written as

$$\begin{aligned} \frac{m_p}{A_p} - \frac{m_r}{A_r} = {} & k_{p+} e^{-\int \frac{b_p}{M_p} dt} \int \frac{1}{M_p} e^{\int \frac{b_p}{M_p} dt} dt + \frac{m_{p0}}{A_p} e^{-\int \frac{b_p}{M_p} dt} \\ & - \left( k_{r+} e^{-\int \frac{b_r}{M_r} dt} \int \frac{1}{M_r} e^{\int \frac{b_r}{M_r} dt} dt + \frac{m_{r0}}{A_r} e^{-\int \frac{b_r}{M_r} dt} \right) \end{aligned} \tag{9}$$

where the subscript $p$ denotes the stressed sample system and the subscript $r$ denotes the reference sample system. An approximation that the sampled volume and the sampling frequency of the stressed sample system are identical to those of the reference sample system gives: $b_p = b_r$ and $M_p = M_r$. By using these approximations, we

can simplified Eq. (9) into

$$\left(\frac{m_p}{A_p}-\frac{m_r}{A_r}\right)e^{\int\frac{b_p}{M_p}dt}=\left(k_{p+}-k_{r+}\right)\int\frac{1}{M_r}e^{\int\frac{b_p}{M_p}dt}dt+\left(\frac{m_{p0}}{A_p}-\frac{m_{r0}}{A_r}\right) \tag{10}$$

We will define $k'_{PS+}$ by the difference between the two experimental dissolution constants of $k_{p+}$ and $k_{r+}$:

$$k'_{PS+} \equiv k_{p+} - k_{r+} \tag{11}$$

We understand that $k'_{PS+}$ is the apparent rate constant of PS reaction (mol/cm$^2$/sec) because an actual reactive area of PS is unknown. Substituting Eq. (11) into Eq. (10) gives

$$\left(\frac{m_p}{A_p}-\frac{m_r}{A_r}\right)e^{\int\frac{b_p}{M_p}dt}=k'_{PS+}\int\frac{1}{M_p}e^{\int\frac{b_p}{M_p}dt}dt+\left(\frac{m_{p0}}{A_p}-\frac{m_{r0}}{A_r}\right) \tag{12}$$

The two values of interfacial areas of $A_p$ and $A_r$ can be replaced approximately by $A = 3Wr^{-1}\rho^{-1}$. The apparent rate constant of PS reaction ($k'_{PS+}$) defined by Eq. (11) can be evaluated by fitting the experimental data to Eq. (12) using the method of weighted least squares.

### 4.2. Dissolution rate and activation energy of the reference sample

The solubility of amorphous silica at 35°C, 45°C, and 55°C under atmospheric pressure were computed using a regression formula as a function of the temperature reported by Rimstidt and Barnes (1980) to be $2.3 \times 10^{-3}$, $2.8 \times 10^{-3}$, and $3.3 \times 10^{-3}$ mol/kg, respectively. Compared to the Si concentration levels of $10^{-4}$ to $10^{-5}$ mol/kg (Fig. 2-a~c) in our experiments, it is obvious that all dissolution experiments of glass beads were carried out under far from equilibrium conditions. Hence, the precipitation rate could be considered as negligible when compared with the dissolution rate in the kinetic calculation. The dissolution rate constant $k_+$ in Eq. (8) (mol/cm$^2$/sec) of the reference sample at each temperature was as follows: $11.6 \pm 0.3 \times 10^{-15}$ (35°C), $32 \pm 1 \times 10^{-15}$ (45°C), and $95 \pm 1 \times 10^{-15}$ (55°C), which were calculated from all the data points plotted after the timing of applying loads in the accompanying stressed systems (Fig. 2). The logarithm of dissolution rate constant was plotted against the reciprocal temperature for the reference samples in the Arrhenius-type one in Fig. 6. The activation energy of dissolution reaction silica in soda-lime glass was obtained from the slope in Fig. 6 to be 89 ± 1 kJ/mol. Perera *et al.* (1991) reported an activation energy of 84 kJ/mol for soda-lime glass dissolution with pH = 8.18. In the every experiment, the solutions had been buffered with respect to pH, however, the final pH values were approximately 0.5 higher than initial ones. The dissolving constituents of the glass could have influenced the dissolution rate. Even though our experiments were carried out at relatively high pH conditions, our result showed good agreement with their value.

### 4.3. Dissolution rate and activation energy of PS reaction

According to the calculation method described in section 4.1 (Eq. (9) to (12)), the dissolution rates of PS reaction at each temperature were estimated on the simple

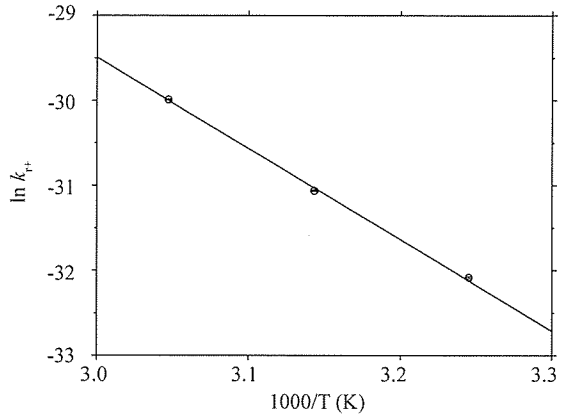


**Fig. 6:** Arrhenius plot of the experimental data for reference samples without load, which suggests an activation energy of 89 ± 1 kJ/mol for dissolution of $SiO_2$. Error bars represent 1 σ of standard error.

assumption that PS reaction accelerates silica dissolution just after applying loads and the PS dissolution rate does not change with time. The data used for the calculation in each temperature were as follows: during the period from the elapsed time (hours) of 261.5 to 447 (35°C), 292 to 430.5 (45°C), and 167.5 to 233 (55°C) in Fig. 3(a), (b), and (c), respectively. The calculated rates were apparent rate constants of PS (mol/cm²/sec) (Eq. (11)), and they were 6 ± 2 × $10^{-15}$ (35°C), 17 ± 4 × $10^{-15}$ (45°C), and 38 ± 17 × $10^{-15}$ (55°C), respectively. Ratios of the rates of PS relative to those of reference samples were 0.5 ± 0.2 (35°C), 0.5 ± 0.1 (45°C), and 0.4 ± 0.2 (55°C), respectively, and also the dissolution rates of stressed samples to those of reference ones were 1.5 ± 0.5 (35°C), 1.5 ± 0.4 (45°C) and 1.4 ± 0.6 (55°C).

Si concentration differences at 45°C and 55°C (Fig. 3b and c) increased even after removing the loads, while Si concentration at 35°C showed flat pattern against to the elapsed time. Increasing rates of Si after unloading were seemed to have different slopes from those of PS reaction. The removal of loads may alter the contact conditions on grain boundaries: solid/solid contact conditions at the time of loading change into solid/fluid contact ones after the removal of load. On such surface areas of newly created solid/fluid contact, it is likely that the once strained surface parts dissolve into solution. The apparent dissolution rates (mol/cm²/sec) for the data obtained after the removal of loads were also calculated assuming that the Si concentrations have increased linearly. The results were −0.2 ± 1.4 × $10^{-15}$ (35°C), 7.4 ± 1.2 × $10^{-15}$ (45°C) and 18 ± 1 × $10^{-15}$ (55°C), respectively. These results are summarized in Table 2, along with PS reaction rates estimated above.

The Arrhenius plot of the dissolution rates of PS reaction ($k'_{PS+}$) was given by Fig. 7. An apparent activation energy of PS dissolution of soda-lime-glass was obtained from the slope of Fig. 7, and the result was 78 ± 12 kJ/mol (1 standard error). This value was almost same as the activation energy of reference sample dissolution at zero effective stress. This result indicates that the dissolution mechanisms of both

**Table 2** Rate constants of dissolution of soda-lime glass.

| Temperature (°C) | Stressed or reference #1 | Effective stress (Mpa) | Rate constant (mol/cm²/sec) #2 | Data used for the calculation |
|---|---|---|---|---|
| 35 | Ref. | 0 | $11.6 \pm 0.3 \times 10^{-15}$ | #3 |
| 35 | PS (St. - Ref.) | 0.05 | $6 \pm 2 \times 10^{-15}$ | during the period from elapsed time of 261.5 to 447 hours in Fig. 3a |
| 35 | after unloading (St. - Ref.) | 0 | $-0.2 \pm 1.4 \times 10^{-15}$ | #4 |
| 45 | Ref. | 0 | $32 \pm 1 \times 10^{-15}$ | #3 |
| 45 | PS (St. - Ref.) | 0.05 | $17 \pm 4 \times 10^{-15}$ | during the period from elapsed time of 292 to 430.5 hours in Fig. 3b |
| 45 | after unloading (St. - Ref.) | 0 | $7.4 \pm 1.2 \times 10^{-15}$ | #4 |
| 55 | Ref. | 0 | $95 \pm 1 \times 10^{-15}$ | #3 |
| 55 | PS (St. - Ref.) | 0.05 | $38 \pm 17 \times 10^{-15}$ | during the period from elapsed time of 167.5 to 233 hours in Fig. 3c |
| 55 | after unloading (St. - Ref.) | 0 | $18 \pm 1 \times 10^{-15}$ | #4 |

#1 "Stressed sample system" and "reference sample system" are denoted as "St." and "Ref.", respectively.
#2 The error is 2 σ of the standard error.
#3 The rate constants of "reference" were calculated using the data points of the reference sample system which were plotted after the timing of applying loads.
#4 The results of "after unloading" were calculated using the data points plotted after the removal of loads in Fig. 3.

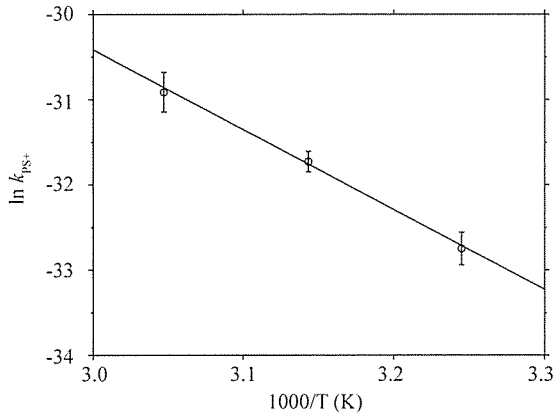


**Fig. 7:** Arrhenius plot of the dissolution rates of pressure solution for 35°C, 45°C and 55°C in this study. Error bars represent 1 σ of standard error.

reactions were basically same. Si release from PS reaction in solution can be detected even at low temperature and low differential stress.

Finally, the influence of very small effective stress on the silica dissolution was discussed. Even though calculated effective stress was very small, an actual applied differential stress at contact surface of glass beads was probably significantly large compared to the practical calculation because of very small contact area of beads. Therefore, stress concentration on the contact point may enhance the dissolution reaction even under apparently low effective stress condition.

## 5. CONCLUSIONS

Dissolution rates of pressure solution (PS) of soda-lime glass at low temperatures (35° to 55°C) and low effective stresses (0.05 MPa) under the condition far from equilibrium have been determined using 0.002 M $NaHCO_3$ solution, and calculation method of dissolution rate in the case of decreasing water mass has been developed on the basis of the kinetics of silica-water reactions. The dissolution rate of Si in the PS reaction was obviously half of that at effective stress = 0. The activation energy of PS reaction of soda-lime glass was 78 ± 12 kJ/mol showing good agreement with that of normal dissolution of approximately 89 kJ/mol within analytical errors. Hence, a reaction mechanism of PS may be the same with that of normal dissolution. The results indicate that Si release from PS reaction into solution can be detected even at such low temperatures and low effective stresses. Since the most water-soluble silica derived from soda-lime glass showed clear PS response to step-like loading, other silica polymorphs such crystalline quartz may also show detective PS response even at the low temperatures and the low effective stresses. This possibility is to be examined in view of the geochemical earthquake prediction by monitoring of the Si concentration in spring waters issuing from granitic basement rocks.

## ACKNOWLEDGMENTS

We are most grateful to Dr. J. H. Choi (Okayama Univ.) for constructive discussion. We would also like to express our thanks to Dr. A. Yoneda (Okayama Univ.) and Dr. T. Iwatsuki (JAEA) for their critical review of the manuscript. We thank Dr. I. Suto (Nagoya Univ.) for SEM observation.

## REFERENCES

Bernabé, Y., Evans, B., Fitzenz, D.D. (2009) Stress transfer during pressure solution compression of rigidly coupled axisymmetric asperities pressed against a flat semi-infinite solid. *Pure Appl. Geophys.* **166**, 899–925.

de Boer, R.B. (1977a) On the thermodynamics of pressure solution-interaction between chemical and mechanical forces. *Geochim. Cosmochim. Acta.* **41**, 249–256.

de Boer, R.B. (1977b) Pressure solution: theory and experiments. *Tectonophysics.* **39**, 287–301.

Dewers, T., Hąjash, A. (1995) Rate laws for water-assisted compaction and stress-induced water-rock interaction in sandstones. *J. Geophys. Res.* **100**, 13093–13112.

Eyring, H. (1935) The activated complex in chemical reactions. *J. Chem. Phys.* **3**, 107.

He, W., Hąjash, A., Sparks, D. (2003) Creep compaction of quartz aggregates: effects of pore-fluid flow – a combined experimental and theoretical study. *Am. J. Sci.* **303**, 73–93.

He, W., Hajash, A., Sparks, D. (2007) Evolution of fluid chemistry in quartz compaction systems:

experimental investigations and numerical modeling. *Geochim. Cosmochim. Acta.* **71**, 4846–4855.

Ichikawa, Y., Choi, J.H., Tanno, T., Hirano, T., and Matsui, H. (2011) Theoretical study of rock for estimating long-term behavior (FY2009) (Contract Research). *Japan Atomic Energy Agency, JAEA research report* **2011–007** (in Japanese with English abstract).

McClay, K.R. (1977) Pressure solution and coble creep in rocks and minerals: a review. *J. Geol. Soc. London* **134**, 57–70.

Perera, G., Doremus, R.H., and Lanford, W. (1991) Dissolution rates of silicate glasses in water at pH 7. *J. Am. Ceram. Soc.* **74**, 1269–1274.

Renard, F., Park, A., Ortoleva, P., Gratier, J.P. (1999) An integrated model for transitional pressure solution in sandstones. *Tectonophysics* **312**, 97–115.

Rimstidt, J.D., Barnes, H.L. (1980) The kinetics of silica-water reactions. *Geochim. Cosmochim. Acta.* **44**, 1683–1699.

Schutjens, P.M.T.M. (1991) Experimental compaction of quartz sand at low effective stress and temperature conditions. *J. Geol. Soc. London* **148**, 527–539.

Scholz, C.H. (2002) *The Mechanics of Earthquakes and Faulting, second ed.* Cambridge Univ. Press, New York. 496 pp.

Shimizu, I. (1995) Kinetics of pressure solution creep in quartz: theoretical considerations. *Tectonophysics* **245**, 121–134.

Yang, T. (2011) Pressure solution of soda-lime glass under effective stress at 25°C to 55°C: The possibility of earthquake prediction by the change of silica concentration in groundwater. *Master thesis, Department of Earth and Planetary Sciences, Graduate School of Environmental Studies, Nagoya University.* 36pp.